Journal of
Nanoscience and Nanotechnology
Vol. 10, 5413–5417, 2010

Structures and Magnetic Properties of Fe_nB ($n = 1$–12) Clusters

Jing Wang[1,2], Ying Liu[1,2,*], Qing-Min Ma[1], and Zun Xie[1]

[1] *Department of Physics, and Hebei Advanced Thin Film Laboratory, Hebei Normal University, Shijiazhuang 050016, Hebei, China*
[2] *National Key Laboratory for Materials Simulation and Design, Beijing 100084, China*

The configurations, electronic structures and magnetic properties of Fe_nB ($n = 1$–12) clusters have been calculated within the framework of all-electron density functional theory. The calculated results indicate that the B atom prefers a surface site for all the lowest-energy structures of Fe_nB with $n = 1$–9 and 11, while for $Fe_{10}B$ and $Fe_{12}B$, the B atom is found to occupy a center site forming a B-centered Fe_n cage. Furthermore, relatively large HOMO–LUMO gaps are found for Fe_6B and Fe_7B, indicating the chemical inertness of the two isomers. For Fe_4B, and $Fe_{12}B$, the spin magnetic moments of the Fe atom significantly increase, but the spin moments decrease slightly for all the other Fe_nB clusters.

Keywords: Density Functional Theory, Mixed Iron Cluster, Magnetic Property.

1. INTRODUCTION

Over the last several years, free clusters and nanoparticles of many types have been intensively studied both experimentally and theoretically. Transition-metal (TM) clusters, especially Fe_n clusters,[1–9] have been studied extensively due to their central role in magnetism, catalysis and many exotic properties. Their ground-state geometries, electronic structures, optical, magnetic, and thermodynamic properties are clearly size-dependent with a non-linear behavior between the two general limits given by the atomic and the bulk-like behavior. Many of these properties can be changed by doping or mixing with other species. For example, B can greatly improve the features of bulk Fe,[10–12] and Fe–B-based crystalline and amorphous alloys have many useful properties such as ferromagnetism, creep and wear resistance.

Ching et al.[10] reported their calculated results on the band structures of the ferromagnetic compounds FeB, Fe_2B, Fe_3B by using a spin-polarized version of the first-principles self-consistent orthogonalized linear combination of atomic orbitals method. They found that the B atom was an electron accepter and the moment on B was slightly polarized opposite to the Fe moments. Moreover, the equilibrium structures, electronic and magnetic properties of Ni_nB clusters with $n = 1$–8, 12 were studied[13] within the framework of density functional theory (DFT). In addition, Sun and coworkers,[14] based on a linear combination of atomic orbitals approach with density functional formalism, gave an analysis of the structures of small Fe_nB ($n = 1$–6) clusters.

In this paper, we report an extensive search for the lowest-energy structures of Fe_nB ($n = 1$–12) clusters within all-electron DFT. The following section (Section 2) gives a brief description of the theoretical method used in this work. In Section 3, we present the lowest-energy structures for Fe_nB clusters. The electronic structure and magnetic properties are discussed in Section 4. Finally, Section 5 summarizes the main conclusions of our computational results.

2. THEORETICAL METHODS

To determine the lowest-energy structures of the Fe_nB clusters, a number of initial structures based on our previous studies,[9,13–15] have been considered. In the calculations, we first performed symmetry-constrained geometry optimizations to search for low-lying metastable isomers among many possible initial structures. Following optimizations within a given symmetry, the lowest-energy configurations were further refined by continuing the optimization without any symmetry restrictions (C_1 symmetry).

In the electronic structure calculations, the double numerical basis plus polarized functions[16] (DNP) was chosen. The exchange-correlation interaction was treated within the GGA using the BLYP functional.[17]

*Author to whom correspondence should be addressed.

1533-4880/2010/10/5413/005 doi:10.1166/jnn.2010.1956

Furthermore, the accuracy of the present all-electron BLYP computational scheme has been validated by our previous work.[9, 15] Self-consistent-field calculations were carried out with a convergence criterion of 10^{-6} Hartree on the total energy. In the geometry optimization, the convergent thresholds were set to 10^{-4} Hartree/Å for the force, 10^{-4} Å for the displacement, and 10^{-5} Hartree for the energy change. The magnetic moments were evaluated via Mülliken population analysis.[18] All computations have been carried out within all-electron DFT as implemented in the DMOL package.[19, 20]

3. CONFIGURATIONS AND STABILITY

Using the computational scheme described in Section 2, the lowest-energy structures and some interesting low-lying metastable isomers for Fe_nB ($n = 1$–12) clusters are shown in Figure 1.

For FeB, the Fe–B bond is 1.725 Å, which is shorter than that of the Fe dimmer (2.020 Å).[9] It is close to the bond length (1.780 Å) obtained by Sun et al.[14] The lowest-energy structure of the Fe_2B cluster is a triangle with C_s symmetry. The two Fe–B bond lengths are 1.840 Å and 1.922 Å, respectively, and the Fe–Fe bond length is 2.219 Å. An isosceles triangle (C_{2v})[14] is also obtained as a low-lying isomer and the binding energy is only 0.085 eV higher than that of the C_s geometry. Another low-lying isomer is a linear chain ($D_{\infty h}$) with the B atom at the center, which is energetically higher than the lowest-energy structure by 0.440 eV. In the case of Fe_3B, the ground-state structure is a planar kite-like configuration (C_{2v}(I)) with the B atom at the vertex. And the 3D tetrahedron obtained as the most stable structure by Sun et al.[14] is also considered in our calculation. The optimized structure is a C_{3v} configuration and it is 0.092 eV higher in energy than the ground state. For the C_{2v}(II) and C_{2v}(III) geometries, they are also the planar structures but energetically unfavored.

As cluster size increases, three dimensional (3D) configurations prevail and become the lowest-energy structures for Fe_nB clusters with $n \geq 4$. The lowest-energy structure of Fe_4B is a triangular bipyramid, which is in good agreement with the results of Sun et al.[14] All the other structural isomers with C_{2v}(I), C_{4v}, D_{4h}, and C_{2v}(II) symmetries are substantially higher in energy than the ground state. For Fe_5B cluster, a tetragonal bipyramid with the B atom at a vertex is obtained as the ground state. There are also six other low-lying isomers lying 0.142, 0.302, 1.013, 1.173, 1.618, 3.012 eV energy difference above the ground state. Specially, the most stable structure obtained in Ref. [14] is just the fifth low-lying isomer in the present results. In the case of Fe_6B, the ground state is a pentagonal bipyramid with the B atom occupying one of the ring sites, as shown in Figure 1. The next low-lying configuration, 0.498 eV higher in energy, is a face-capped tetragonal bipyramid with C_s symmetry. The third one is a bicapped trigonal bipyramid. Among the eight low-lying isomers obtained, there is a planar hexagon with the B atom at the ring site, which is 3.043 eV higher in energy than the ground state. For $n = 7$, the ground state is a bicapped octahedron with C_s symmetry and the B atom is also on the vertex site. For the other six low-lying isomers, it can be seen that the B atom prefers also to the vertex site.

As to the case of Fe_8B, the lowest-energy structure is a tricapped trigonal prism and the B atom substitutes the cap sites. It is worth mentioning that the next low-lying isomer is a D_{4d} geometry with the B atom at the center, which is 0.311 eV higher in energy than the ground state. The third isomer, as shown in Figure 1, is a C_{2v} configuration with the B atom at the vertex. For Fe_9B, a tetragonal antiprism (C_{4v}) is obtained as the ground state. Moreover, the next low-lying isomer is a C_s configuration with the B atom on the center site, which is energetically higher by 0.319 eV than the ground state. All the other obtained low-lying isomers are structures, in which the B atom occupies the vertex site. For $n = 11$, the lowest-energy structure is an icosahedron with C_{5v} symmetry and the B atom locates at the vertex. There are also two low-lying isomers (C_s and C_2) in which one is with the B atom near the center and the other one is with the B atom on a surface site (C_{3v}). Thus, the doped B atom prefers to occupy the surface sites for $n \leq 9$ and $n = 11$.

It is worth mentioning that the lowest-energy structures of $Fe_{10}B$ and $Fe_{12}B$ clusters are two compact structures, in which the B atom occupies a center site. It is known that the B atom is of small size compared with Fe. Thus the B atom favors to occupy the center site when forming the cage. For $Fe_{10}B$, a D_{4d} geometry is obtained as the ground state. Several other isomers (C_{2v}(I), C_{2v}(II), D_{5d}, C_{5v}) are considered and the B atom prefers an interior site for all these structures except the C_{5v} geometry. The ground state of $Fe_{12}B$ is a B-centered D_{5d} geometry, as shown in Figure 1. However, the following three low-lying isomers with the B atom on the top site are obtained and then there exist other three isomers with the B atom at the center. Energetically, all these six configurations are unfavored.

All the structures of the Fe_nB ($n = 1$–12) clusters can be derived from capping/putting a B atom over/inside the Fe_n clusters. The calculated results indicate that the B atom prefers the surface site for all the lowest-energy structures except the case of $n = 10$ and 12, while for the ground states of $Fe_{10}B$ and $Fe_{12}B$, the B atom occupies a central site. Starting from $n = 4$, the lowest-energy structures begin to adopt the 3D structure.

4. ELECTRONIC STRUCTURE

Upon the doping of the B atom, the binding energy per atom increases and the stability is enhanced for Fe_nB ($n = 1$–12) comparing with pure Fe_n clusters.[9] The gaps

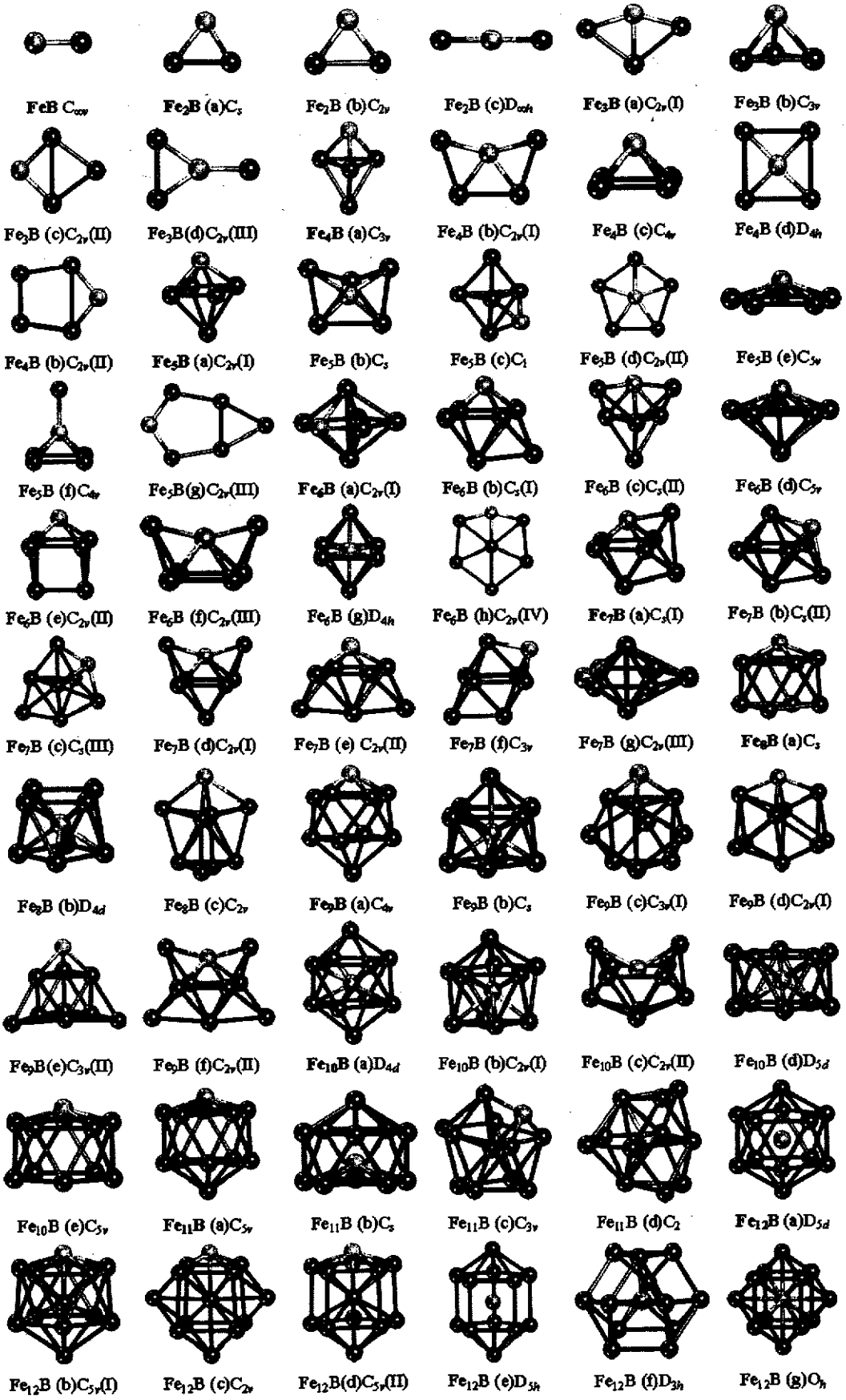

Fig. 1. Ground-state configurations and some low-lying isomers for Fe_nB ($n = 1$–12) clusters. Light ball: B atom; dark ball: Fe atom.

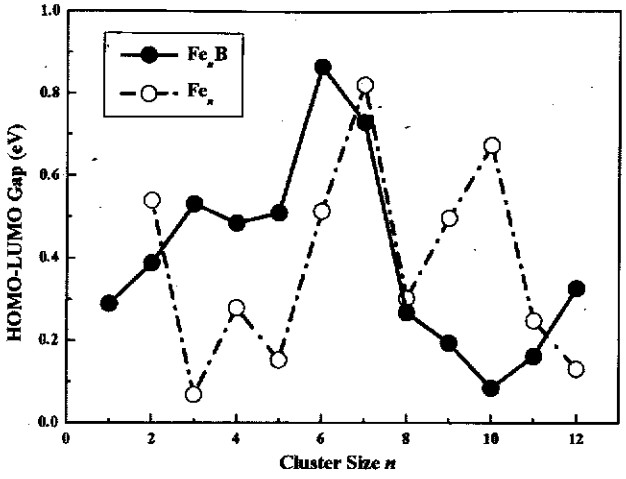

Fig. 2. Size dependence of the HOMO–LUMO gaps of Fe_nB ($n = 1$–12) and pure Fe_n ($n = 2$–12) clusters.

between the highest occupied molecular orbital (HOMO) and the lowest unoccupied molecular orbital (LUMO) and the magnetic moment of the total Fe atoms for Fe_nB are shown in Figures 2 and 3, respectively.

The size dependence of HOMO–LUMO gaps for Fe_nB ($n = 1$–12) is shown in Figure 2. It can be seen that the B-doped clusters have a relatively small gap arranging from 0.084 to 0.899 eV. For Fe_6B and Fe_7B, the HOMO–LUMO gaps are obviously larger than that of the other clusters, which indicates that these two structures are more stable than the other ones. For comparison, the HOMO–LUMO gaps of pure Fe_n clusters are also plotted in Figure 2. We note that the doping of the B atom divides the gaps into four main parts. For $n = 2$, the HOMO–LUMO gap is smaller than that of the pure Fe_2 cluster. For $2 < n \leq 6$, the HOMO–LUMO gaps increase slightly, while the corresponding values reduce for $7 \leq n \leq 11$. Then the gap of $Fe_{12}B$ becomes larger against that of Fe_{12}. The magnetic properties of Fe_nB clusters are also

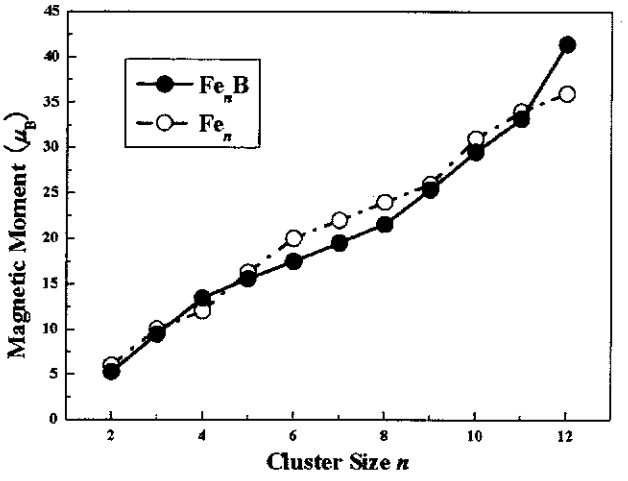

Fig. 3. Magnitudes of spin moment of the total Fe atoms for Fe_nB and pure Fe_n ($n = 2$–12) clusters.

discussed. Figure 3 shows the total spin moments of the Fe atoms for Fe_nB against the cluster size n, where the corresponding values of the pure Fe clusters have also been plotted for comparison. On the whole, the spin magnetic moments of pure Fe_n ($n = 2$–3, 5–11) clusters decrease slightly upon doping a B atom, while for Fe_4B and $Fe_{12}B$ the magnetic moments increase. It is interesting to find out that the difference of the average bond lengths for Fe_4B and Fe_4 are relatively large (0.117 Å), while the value for $Fe_{12}B$ and Fe_{12} can be considered as zero within the calculation precision. Thus, it is the size effect which should contribute to the increase of the magnetic moments for Fe_4B. For $Fe_{12}B$, the increase of the magnetic moment is different from that of Fe_4B. The lowest-energy structure of $Fe_{12}B$ is a B-centered icosahedron with the Fe atoms on the surface sites. Therefore, the surface enhancement effect should be responsible for the increase of the magnetic moment of $Fe_{12}B$.

5. CONCLUSIONS

In summary, using the all-electron DFT-GGA calculation, the lowest-energy structures of Fe_nB ($n = 1$–12) clusters are obtained by considering a large number of structural isomers for each cluster size. The results indicate that the B atom prefers a surface site for all the Fe_nB clusters with $n = 1$–9 and 11, while for $n = 10$ and 12, the B atom occupies a center site. Specially, the transition from 2D configuration to 3D configuration occurs at $n = 4$. Furthermore, the size dependences of the HOMO–LUMO gaps and the spin magnetic moments have also been discussed. Large HOMO–LUMO gaps are found at Fe_6B and Fe_7B, indicating their chemical inertness. The significant increase of the spin magnetic moments of Fe for Fe_4B and $Fe_{12}B$ can be interpreted by two different mechanisms: the size effect for Fe_4B and the surface enhancement effect for $Fe_{12}B$. It is anticipated that all the calculated results will contribute to understand the effect of the B atom on the magnetic properties of the Fe clusters.

Acknowledgments: We would like to thank Professor Chen Nan-Xian and Professor Shen Jiang for helpful discussions. This work was supported by the National Natural Science Foundation of China (Grant No.10874039), the Natural Science Foundation of Hebei Province (No. A2008000134). We gratefully acknowledge financial support from the 973 Project in China under Grant No. 2006CB605101.

References and Notes

1. W. A. de Heer, P. Milani, and A. Chatelain, *Phys. Rev. Lett.* 65, 488 (**1990**).
2. J. Dorantes-Davila, H. Dreysse, and G. M. Pastor, *Phys. Rev. B* 46, 10432 (**1992**).

3. I. M. L. Billas, A. Chatelain, and W. A. de Heer, *Science* 265, 1682 (**1994**).
4. M. Sakurai, K. Watanabe, K. Sumiyama, and K. Suzuki, *J. Chem. Phys.* 111, 235 (**1999**).
5. J. L. Chen, C. S. Wang, K. A. Jackson, and M. R. Pederson, *Phys. Rev. B* 44, 6558 (**1991**).
6. M. Castro and D. R. Salahub, *Phys. Rev. B* 49, 11842 (**1994**).
7. P. Ballone and R. O. Jones, *Chem. Phys. Lett.* 233, 632 (**1995**).
8. O. Dieguez, M. M. G. Alemany, C. Rey, P. Ordejon, and L. J. Gallego, *Phys. Rev. B* 63, 205407 (**2001**).
9. Q. M. Ma, Z. Xie, J. Wang, Y. Liu, and Y. C. Li, *Solid State Commun.* 142, 114 (**2007**).
10. W. Y. Ching, Y. N. Xu, B. N. Harmon, J. Ye, and T. C. Leung, *Phys. Rev. B* 42, 4460 (**1990**).
11. J. Hafner, M. Tegze, and Ch. Becker, *Phys. Rev. B* 49, 285 (**1994**).
12. J. W. Taylor, J. A. Duffy, A. M. Bebb, M. J. Cooper, S. B. Dugdale, J. E. McCarthy, D. N. Timms, D. Greig, and Y. B. Xu, *Phys. Rev. B* 63, 220404 (**2001**).
13. M. Deshpande, D. G. Kanhere, and R. Pandey, *Phys. Rev. A* 71, 063202 (**2005**).
14. Q. Sun, X. G. Gong, Q. Q. Zheng, and G. H. Wang, *J. Phys.: Condens. Matter.* 8, 1805 (**1996**).
15. Q. M. Ma, Z. Xie, J. Wang, Y. Liu, and Y. C. Li, *Phys. Rev. B* 76, 035412 (**2007**).
16. B. Delley, *J. Chem. Phys.* 92, 508 (**1990**).
17. A. D. Becke, *J. Chem. Phys.* 88, 2547 (**1988**); C. Lee, W. Yang, and R. G. Parr, *Phys. Rev. B* 37, 785 (**1988**).
18. R. S. Mulliken, *J. Chem. Phys.* 23, 1841 (**1955**).
19. B. Delley, *J. Chem. Phys.* 92, 508 (**1990**).
20. B. Delley, *J. Chem. Phys.* 113, 7756 (**2000**).

Received: 14 September 2007. Revised/Accepted: 7 June 2008.